Available online at www.sciencedirect.com
SCIENCE DIRECT
Journal of Fluorine Chemistry 126 (2005) 1288–1296
JOURNAL OF FLUORINE CHEMISTRY
www.elsevier.com/locate/fluor

Gas phase UV and IR absorption spectra of $CF_3CH_2CH_2OH$ and $F(CF_2CF_2)_xCH_2CH_2OH$ ($x = 2, 3, 4$)

R.L. Waterland [a,*], M.D. Hurley [b], J.A. Misner [b], T.J. Wallington [b,**], S.M.L. Melo [c], K. Strong [c], R. Dumoulin [c], L. Castera [c], N.L. Stock [d], S.A. Mabury [d]

[a] *DuPont Central Research and Development, E. I. DuPont de Nemours and Co. Inc., P.O. Box 80249, Wilmington, DE 19880-0249, USA*
[b] *Ford Motor Company, P.O. Box 2053, Dearborn, MI 48121-2053, USA*
[c] *Department of Physics, University of Toronto, 60 St George Street, Toronto, ON, Canada M5S 1A7*
[d] *Department of Chemistry, University of Toronto, 80 St George Street, Toronto, ON, Canada*

Received 16 May 2005; received in revised form 23 June 2005; accepted 24 June 2005
Available online 2 August 2005

Abstract

The UV and IR spectra of $CF_3CH_2CH_2OH$ and $F(CF_2CF_2)_xCH_2CH_2OH$ ($x = 2, 3, 4$) were investigated using computational and experimental techniques. Computational methods were used to show that $CF_3CH_2CH_2OH$ and $F(CF_2CF_2)_xCH_2CH_2OH$ ($x = 2, 3$) have UV absorption in the region 140–175 nm. Photolysis is therefore *not* a significant environmental loss mechanism for fluorinated alcohols. Experimental methods were used to record IR spectra for $CF_3CH_2CH_2OH$ and $F(CF_2CF_2)_xCH_2CH_2OH$ ($x = 2, 3, 4$) at spectral resolutions of 0.004–0.5 cm^{-1} with, and without, 700 Torr of air diluent. There was no discernable effect of total pressure or spectral resolution over the range studied. Calculated IR spectra agreed well with those measured experimentally, and were used to assign the IR spectra.

Keywords: Fluorotelomer alcohols; IR measurements; Hydrogen-bonded conformation

1. Introduction

Fluorotelomer alcohols, (FTOHs, $F(CF_2CF_2)_xCH_2CH_2OH$, $x = 2$–8) are chemical intermediates commonly used in the manufacture of fluorotelomer-based products. Although the environmental fate of FTOHs is not fully determined, the atmospheric oxidation of FTOHs has been suggested as a source of long-chain perfluoroalkyl carboxylic acids (PFCAs, $C_xF_{2x+1}COOH$, where $x = 6$–12) observed in remote locations [1–5]. Additional laboratory studies of the atmospheric chemistry of FTOHs are required to confirm or refute these suggestions. A computational and experimental study of the UV and IR spectra of $CF_3CH_2CH_2OH$ and $F(CF_2CF_2)_xCH_2CH_2OH$ ($x = 2$, 3, 4) has been performed to examine the role of photolytic destruction mechanisms, facilitate future laboratory work and permit the possible spectroscopic detection of FTOHs in the atmosphere. Results are reported herein.

2. Experimental and computational details

Samples of the fluorinated alcohols were obtained from commercial sources at stated purities >97%. $CF_3CH_2CH_2OH$, $F(CF_2CF_2)_2CH_2CH_2OH$ and $F(CF_2CF_2)_3CH_2CH_2OH$ are liquids at room temperature and were subjected to freeze-pump-thaw cycling before use. $F(CF_2CF_2)_4CH_2CH_2OH$ is a solid and was used as received.

2.1. IR measurements at Ford

The experimental setup consisted of a Mattson Instruments, Sirius 100 Fourier transform infrared spectrometer,

* Corresponding author. Tel.: +1 3026951511; fax: +1 3026958805.
** Co-corresponding author.
E-mail addresses: robert.l.waterland@usa.dupont.com (R.L. Waterland), twalling@ford.com (T.J. Wallington).

0022-1139/$ – see front matter © 2005 Elsevier B.V. All rights reserved.
doi:10.1016/j.jfluchem.2005.06.010

interfaced to a 140 L, 2 m long evacuable Pyrex chamber described elsewhere [6]. The spectrometer was operated at a spectral resolution of 0.50 cm^{-1}. Infrared spectra were derived from 32 co-added interferograms. Spectra were recorded at 296 K in the presence of 700 Torr of air diluent.

$CF_3CH_2CH_2OH$ and $F(CF_2CF_2)_2CH_2CH_2OH$ have substantial (>1 Torr) vapor pressures; gas mixtures containing known partial pressures of these compounds can be prepared using standard techniques. $F(CF_2CF_2)_3CH_2CH_2OH$ and $F(CF_2CF_2)_4CH_2CH_2OH$ have lower vapor pressures (<0.2 Torr) and it is difficult to prepare *quantitative* standard mixtures of these compounds using conventional capacitance manometers. $F(CF_2CF_2)_3CH_2CH_2OH$ was admitted into the chamber by allowing the vapor above the liquid to fill a calibrated volume, the contents of which were subsequently swept into the chamber with air diluent. $F(CF_2CF_2)_4CH_2CH_2OH$ was admitted into the chamber by flowing air diluent over the solid sample and into the chamber. Calibration of the quantity of $F(CF_2CF_2)_3CH_2CH_2OH$ and $F(CF_2CF_2)_4CH_2CH_2OH$ in the chamber was achieved in an indirect fashion. Molecular chlorine was added to the gas mixtures, the mixtures were irradiated with UV light, and the loss of FTOH was equated to the formation of HCl (measured using a calibrated HCl reference spectrum).

We estimate the absorption cross section measurements for $CF_3CH_2CH_2OH$ and $F(CF_2CF_2)_2CH_2CH_2OH$ to be accurate to within ±5% [6], while those for $F(CF_2CF_2)_3CH_2CH_2OH$ and $F(CF_2CF_2)_4CH_2CH_2OH$ are estimated to be accurate to within ±10%. As a check of our experimental technique, the indirect calibration methodology was applied to $F(CF_2CF_2)_2CH_2CH_2OH$ and returned an integrated absorption cross section within 5% of that measured using the direct approach.

2.2. IR measurements at Toronto

The experimental setup at the University of Toronto consisted of a Bomem DA8 Fourier transform spectrometer equipped with a KBr beam-splitter and a MCT detector covering the spectral range of 900–3500 cm^{-1}. The spectrometer was interfaced to a 25 cm long stainless steel cell, equipped with ZnSe windows. Spectra were derived from 350 co-added interferograms taken at a spectral resolution of 0.50 cm^{-1}. The measurements were made at 296 K using samples of pure compounds. High-resolution (0.017 and 0.004 cm^{-1}) spectra were taken to search for fine structure in the IR spectrum; none was observed.

The measurements at Toronto were performed using low pressures (<2.0 Torr) of pure samples without diluent gas. $F(CF_2CF_2)_4CH_2CH_2OH$ had insufficient vapor pressure to be studied using the system at Toronto. We estimate the accuracies of the cross sections derived from these spectra to be comparable to those of the Ford data: 5% for $CF_3CH_2CH_2OH$ and $F(CF_2CF_2)_2CH_2CH_2OH$, and 10% for $F(CF_2CF_2)_3CH_2CH_2OH$. The measurements exhibited only small random errors; the standard deviation on the average cross section in the regions of maximum absorption were found to be 2% for $CF_3CH_2CH_2OH$ (using eight independent cross section measurements) and $F(CF_2CF_2)_2CH_2CH_2OH$ (using six cross sections) and 3% for $F(CF_2CF_2)_3CH_2CH_2OH$ (using 14 cross sections).

2.3. Computational study at DuPont

2.3.1. FTOH conformations and intramolecular hydrogen bonding

There have been three recent experimental determinations of FTOH vapor pressure [7–9]. In Stock et al. [7], it was suggested that the perfluorinated alkyl chain and an intramolecular hydrogen bond between the fluorines and the alcohol moiety contributed to the high volatility of FTOHs. Similar vapor pressure values were reported for the 4-2 to 10-2 FTOHs [10] in a subsequent work by Lei et al. [8] using a different experimental method.

More recently [9], an experimental study of FTOH vapor pressures in the temperature range from 21 to 250 °C showed significantly lower (~10–13 times) vapor pressures than those of Stock [7] and Lei [8]. Furthermore, no empirical evidence was found to support the existence of substantial intramolecular hydrogen bonding in the gas phase. However, ab initio calculations for $F(CF_2CF_2)CH_2$-CH_2OH (2-2 FTOH) and $F(CF_2CF_2)_2CH_2CH_2OH$ (4-2 FTOH) did predict a weak intramolecular hydrogen bonding interaction of the order of 1.5 kcal/mol, in agreement with several related molecular systems reported in the literature [11–18]. In what follows, we have further investigated weak FTOH bonding.

Krusic et al. [9], using the same level of calculation as the present work, showed that extending the length of the perfluorinated tail from two carbons (2-2 FTOH) to four carbons (4-2 FTOH) has almost no effect on the relative energy of the FTOH rotomers; in both cases, the intramolecular hydrogen-bonded conformer is the lowest energy conformation and the binding energy is about 1.4 kcal/mol. Thus, addition of a CF_2CF_2 moiety far from the C–H bonds that participate in intramolecular bonding does not appear to change hydrogen bond energetics. This result will also apply for the longer FTOHs studied in this work, $F(CF_2CF_2)_3CH_2CH_2OH$ (6-2 FTOH) and $F(CF_2$-$CF_2)_4CH_2CH_2OH$ (8-2 FTOH). Accordingly, we have assumed the hydrogen-bonded conformation to be the ground state molecular structure for both 6-2 FTOH and 8-2 FTOH and all results reported below for these molecules are for this conformation.

However, for the smallest FTOH studied here, $CF_3CH_2CH_2OH$, the presence of a terminal F atom rather than a $–CF_2–$ unit may change the relative ordering of the various rotational conformations. Hence, we have examined the important rotational conformations of $CF_3CH_2CH_2OH$. As will be shown, the structures and relative enthalpies of

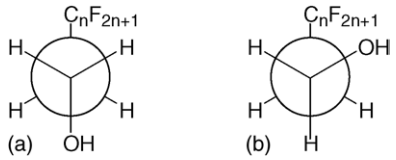

Fig. 1. Newman projections corresponding to rotation about the C_α–C_β single bond in linear FTOHs; (a) is the *anti* conformer and (b) is one of the two equivalent *gauche* conformers.

these conformations are entirely consistent with those previously obtained by Krusic et al. [9].

The important conformations are the *anti* and *gauche* forms illustrated by the Newman projections in Fig. 1. These conformations correspond to rotation about the C_α–C_β single bond. The *gauche* conformation brings a fluorine atom and the hydroxyl group into closest proximity and affords the best chance of forming an intramolecular C–F. . .H–O hydrogen bond.

In Fig. 2, we have sketched the three important molecular conformations for linear FTOHs. Structure (a) shows the extended *anti* form. For linear non-halogenated alcohols, the *anti* form is known to be the lowest energy conformation. Structure (b) shows the *gauche* conformation related to the *anti* form by a 120° rotation around the C_α–C_β single bond. Finally, structure (c) shows the likely conformation of the proposed hydrogen-bonded six-membered ring structure. In Sections 3.2 and 3.3 of this paper, we will refer to these conformations as "*anti*", "*gauche*" and "*bonded*", respectively.

An accurate description of hydrogen bonding requires a careful treatment of electron correlation. Conventional Hartree–Fock based correlation methods such as coupled-cluster theory [19] provide excellent descriptions of correlation effects but, due to their high computational expense, these methods are limited to the smallest of molecules. In contrast, density functional theory (DFT) incorporates a sophisticated electron correlation treatment in a calculation little more expensive than the Hartree–Fock method [20], and over the past few years, DFT has become the method of choice for small to medium sized hydrogen-bonded systems [21–23].

In a careful study of 53 hydrogen-bonded complexes, Rablen et al. [24] demonstrated that a combination of the hybrid DFT method B3LYP [25] with basis sets that include diffuse polarization functions provides a reliable means for determining hydrogen bond strengths.

The specific recommendation in Rablen et al. [24] was to use B3LYP/6-31+G(d(X+),p) for geometry optimization and B3LYP/6-31++G(2d(X+),p) for single point energy calculations [26]. For this study, we used a combination of B3LYP with significantly larger basis sets. All structures were optimized with B3LYP/6-31+G(d,p) and harmonic vibrational frequencies were calculated at the optimized geometries using the same method to ensure that true minima had been obtained. Single point energy calculations were performed on these optimized geometries using B3LYP/6-311++G(3df,2p). All ab initio calculations were carried out using the Gaussian 03 suite of programs [27].

2.3.2. Computation of FTOH ultraviolet and infrared spectra

Time-dependent density functional theory (TD-DFT) is the standard method for rapid and accurate prediction of the properties of electronically excited states and for the estimation of UV and visible spectra. In the last few years, TD-DFT has been used to predict UV and visible spectra for a variety of molecular species [28–34]. Comparison of calculated and experimental transition energies and oscillator strengths shows that TD-DFT significantly outperforms older Hartree–Fock based methods such as configuration interaction singles (CIS) [35]. Matsuzawa et al. [36] and Waterland et al. [37] have demonstrated that TD-DFT calculations of photoabsorption spectra that incorporate empirical correction of the transition energies are particularly useful. Hashikawa et al. [38] have recently used the same approach to estimate photoabsorption spectra for a homologous series of perfluorinated aldehydes. Theory and experiment showed good agreement.

In the present work, the UV spectra calculations were also performed using the Gaussian 03 suite of programs [27]. We used the gradient-corrected level of density functional theory utilizing Becke's three-parameter exchange functional [39] and the Lee–Yang–Parr correlation functional [40] (B3LYP).

Molecular geometries were optimized using the DFT-derived DZVP basis set [41] and the same basis set was used for frequency calculations to ensure that computed geometries corresponded to bound molecular states. Vertical excitation energies and oscillator strengths were calculated with TD-DFT. These calculations employed 12 excited states and used the DZVP basis set augmented with Dunning and Hay's Rydberg functions [42] on all heavy atom centers.

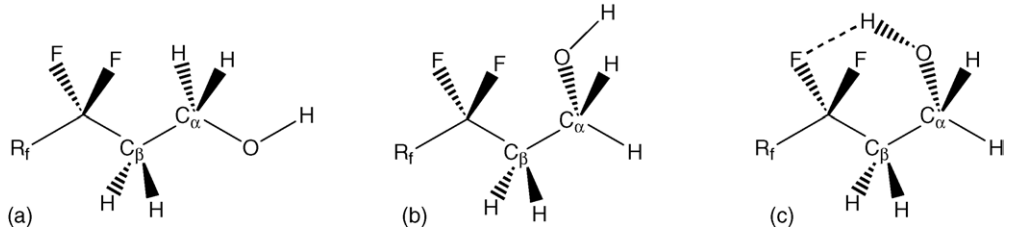

Fig. 2. The three important molecular conformations for linear FTOHs.

We incorporated energy re-scaling in the same manner as Matsuzawa et al. [36] and Waterland et al. [37]. As in our previous work, we used the correlation expression:

$$E_{expt} = 1.144E_{calc} - 0.553\,eV.$$

This expression was developed by fitting the experimental spectra of formaldehyde, benzene and methane; the fitting R^2 was 0.961.

For the estimation of IR spectra, we re-optimized all molecular geometries using B3LYP with the 6-31G* basis set [27] and computed harmonic vibrational frequencies and intensities at the same level of theory on the resultant optimized geometries. Vibrational frequencies were scaled by 0.961 as recommended by Scott and Radom [43].

3. Results

3.1. Measured IR spectra

IR spectra of $CF_3CH_2CH_2OH$, $F(CF_2CF_2)_2CH_2CH_2OH$ and $F(CF_2CF_2)_3CH_2CH_2OH$ were measured at Ford and Toronto. The IR spectrum of $F(CF_2CF_2)_4CH_2CH_2OH$ was measured at Ford. Spectra were recorded using spectral resolutions of 0.004, 0.1 and 0.5 cm^{-1} in the presence and absence of 700 Torr of air diluent at 296 K. There was no discernable effect (<10%) of spectral resolution or the presence of diluent gas on the IR spectra. The Ford and Toronto absorption cross sections agreed to within 2% for $CF_3CH_2CH_2OH$ and 10% for $F(CF_2CF_2)_2CH_2CH_2OH$. The typical accuracy associated with measurements of IR spectra for volatile gases (determined by uncertainties associated with sample concentration, IR pathlength and spectrum noise) is approximately ±5% [44]. The Ford and Toronto spectra for $CF_3CH_2CH_2OH$ and $F(CF_2CF_2)_2CH_2CH_2OH$ are in agreement within the combined experimental uncertainties. For $F(CF_2CF_2)_3CH_2CH_2OH$, there was no discernable difference in the shape of the spectra, but the measured absorption cross sections differed in magnitude. Over the range 600–2000 cm^{-1}, there was a mean difference of 27% between the absorption cross sections measured at Ford and Toronto. This difference indicates the presence of significant systematic error in at least one of the studies. The discrepancy presumably reflects difficulties associated with handling this lower volatility compound. Efforts to resolve the discrepancy were not successful. There being no obvious reason to prefer one laboratory over the other, we choose to cite spectra for $CF_3CH_2CH_2OH$, $F(CF_2CF_2)_2CH_2CH_2OH$ and $F(CF_2CF_2)_3CH_2CH_2OH$ shown in Fig. 3, which are averages of the spectra measured at Ford and Toronto. The spectrum of $F(CF_2CF_2)_4CH_2CH_2OH$ shown in Fig. 3 was acquired at Ford (this compound was not studied at Toronto).

The infrared spectrum of $CF_3CH_2CH_2OH$ has absorption features at 1139 and 1260 cm^{-1} with absorption cross sections of 1.08×10^{-18} and 9.47×10^{-19} cm^2 $molecule^{-1}$;

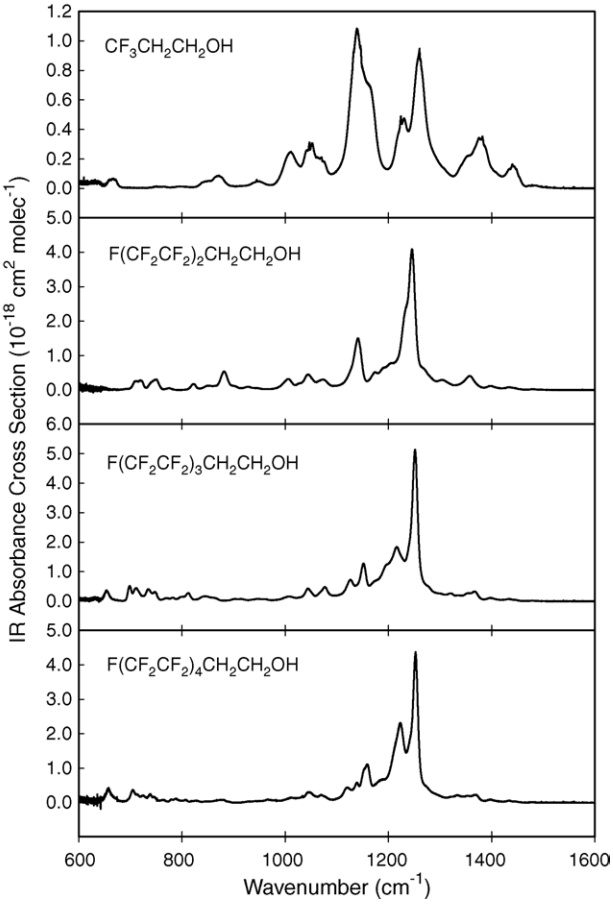

Fig. 3. Measured IR spectra for $CF_3CH_2CH_2OH$, $F(CF_2CF_2)_2CH_2CH_2OH$, $F(CF_2CF_2)_3CH_2CH_2OH$ and $F(CF_2CF_2)_4CH_2CH_2OH$.

$F(CF_2CF_2)_2CH_2CH_2OH$ has absorption features at 1141 and 1246 cm^{-1} with absorption cross sections of 1.50×10^{-18} and 4.03×10^{-18} cm^2 $molecule^{-1}$; $F(CF_2CF_2)_3CH_2CH_2OH$ has absorption features at 1216 and 1251 cm^{-1} with absorption cross sections of 1.83×10^{-18} and 5.11×10^{-18} cm^2 $molecule^{-1}$. The infrared spectrum of $F(CF_2CF_2)_4CH_2CH_2OH$ has absorption features at 1159 and 1253 cm^{-1} with absorption cross sections of 1.1×10^{-18} and 4.3×10^{-18} cm^2 $molecule^{-1}$. In light of the discussion above, we choose to cite uncertainties of ±10% for the smallest two and ±20% for the largest two molecules, respectively.

3.2. Calculated molecular geometries and relative enthalpies

In Table 1, we have listed the calculated relative enthalpies of the "*anti*", "*gauche*" and "*bonded*" conformations of $CF_3CH_2CH_2OH$. The "*anti*" conformer has C_s symmetry and the "*gauche*" and "*bonded*" conformers are both C_1. The B3LYP/6-31+G(d,p) optimized geometries are given in cartesian co-ordinate form in the supplementary material. The reported enthalpies are relative to the "*anti*" conformation and the values are ideal gas enthalpy differences at

Table 1
Relative molar enthalpy[a] (kcal/mol) of the three critical conformations of $CF_3CH_2CH_2OH$ (the 1-2 FTOH), $CF_3CF_2CH_2CH_2OH$ (the 2-2 FTOH) and $CF_3(CF_2)_3CH_2CH_2OH$ (the 4-2 FTOH)

Species	*Anti*	*Gauche*	*Bonded*
1-2 FTOH	0	+1.03	−0.32
2-2 FTOH	0	+1.10	−0.35
4-2 FTOH	0	+1.10	−0.37

[a] Calculational method used B3LYP/6311++G(3df,2p)//B3LYP/6-31+G(d,p). Enthalpies reported at 298.15 K and 1 atm.

Table 2
Relative molar Gibbs Free Energy[a] (kcal/mol) of the three critical conformations of $CF_3CH_2CH_2OH$ (the 1-2 FTOH), $CF_3CF_2CH_2CH_2OH$ (the 2-2 FTOH) and $CF_3(CF_2)_3CH_2CH_2OH$ (the 4-2 FTOH)

Species	*Anti*	*Gauche*	*Bonded*
1-2 FTOH	0	+1.06	+0.18
2-2 FTOH	0	+0.99	+0.31
4-2 FTOH	0	+1.10	+0.28

[a] Calculational method used B3LYP/6-311++G(3df,2p)//B3LYP/6-31+G(d,p). Molar Gibbs Free Energies reported at 298.15 K and 1 atm.

298.15 K and 1 atm corrected for zero-point energy differences. For comparison purposes, we have also shown in Table 1 the corresponding relative enthalpies for the 2-2 and 4-2 FTOHs obtained by Krusic et al. [9]. For all of these FTOHs, the hydrogen-bonded conformation (''*bonded*'') is the lowest enthalpy state, that is a hydrogen bond is predicted to exist, and, as expected, the ''*gauche*'' conformer is the least stable.

The C–F. . .H–O hydrogen bonds are weak. A sensible definition of the bond strength is the calculated enthalpy of the ''*bonded*'' conformation relative to that of the ''*gauche*'' form. On this measure, the calculated bond strength of $CF_3CH_2CH_2OH$ is 1.35 kcal/mol which should be compared to 1.45 kcal/mol for 2-2 FTOH and 1.47 kcal/mol for the 4-2 FTOH. Since the ''*bonded*'' conformation is in all cases the energetically preferred state, we chose it as the basis for our calculations of the UV and IR spectra.

Apart from the work of Krusic et al. [9], there are no previous intramolecular C–F. . .H–O hydrogen bonding calculations for molecules that incorporate a $–CH_2CH_2OH$ moiety. Related systems have been studied. Marler et al. [11] found an experimental intramolecular bond strength of 1.4 kcal/mol for *o*-trifluoromethylphenol. Several groups have examined intramolecular hydrogen bonding in CH_2FCH_2OH: Dixon and Smart [12] obtained a hydrogen bond strength of 1.9 kcal/mol at the MP2 level using a triple-ζ basis set with two sets of polarization functions on C, F and O and one set of polarization functions on H. This result agrees well with the experimental value (2.07 ± 0.53 kcal/mol) obtained from band intensities in CCl_4 [13]. Briggs et al. [16] studied the same system using B97-2/TZVP and reported an essentially identical bond strength of 2.0 kcal/mol. Wiberg and Murcko [14] also studied CH_2FCH_2OH and obtained bond strengths of 2.24 and 2.30 kcal/mol at the MP2/6-311G(d,p)//MP2/6-31G(d) level, respectively, and almost the same results using MP3/6-311G(d,p)//MP2/6-31G(d). Bako et al. [15] examined intramolecular hydrogen bonding in CF_3CH_2OH and found bond strengths of 1.39 and 1.70 kcal/mol at the B3LYP/6-311+G(d,p) and MP2/6-311+G(d,p) level of theory, respectively. Finally, Kovas et al. [17] found an anomalously high bond strength of 2.92 kcal/mol for 2-fluorophenol using MP2/6-31+G(d,p)//MP2/6-31G(d,p) which agrees poorly with the experimental value of 1.63 ± 0.07 kcal/mol reported by Carlson et al. [18]. With the exception of Kovacs et al., these results, those of Krusic et al. [9] and the current work are consistent with the notion that intramolecular C–F. . .H–O hydrogen bonding is weak. Computed and experimental bond strengths lie in the range of 1.3–2.3 kcal/mol and the hydrogen bonds substantially weaken with increasing F substitution.

Our computational results are only directly applicable to the gas phase, but we note that in the condensed phase, these weak *intra*molecular bonds will be overwhelmed by the much stronger *inter*molecular bonding characteristic of alcohols [45]. For a pure component FTOH gas, the partitioning among the three conformers is determined by the relative molar Gibbs Free Energies. In Table 2, we report the molar Gibbs Free Energies relative to the ''*anti*'' conformation at 298.15 K and 1 atm. For all of the FTOHs studied, the ''*anti*'' form is the preferred conformation but the Gibbs Free Energy difference between the ''*anti*'' and ''*bonded*'' conformers is indistinguishable from zero given the expected accuracy of the method used here. We conclude that both conformers will be present at 298.15 K in the gas phase. A more representative atmospheric temperature is 277 K: the calculated relative molar Gibbs Free Energies at this temperature are almost indistinguishable from the values given in Table 2.

3.3. Calculated UV spectra

The ground electronic state is ^1A for all four species studied in this paper. SCF convergence problems prevented us from computing the vertical transition energies and oscillator strengths for $CF_3(CF_2)_7CH_2CH_2OH$.

In Table 3, we show the wavelength and oscillator strength for the first 12 electronic transitions (singlet or triplet) of $CF_3CH_2CH_2OH$, $F(CF_2CF_2)_2CH_2CH_2OH$ and $F(CF_2CF_2)_3CH_2CH_2OH$. These transitions include all those with wavelengths greater than 150 nm. Since the solar spectrum below 290 nm is completely absorbed by stratospheric trace gases, a necessary condition for photolysis in the troposphere is that the compound absorb UV at wavelengths above 290 nm. We have included lower wavelengths for completeness.

Singlet–triplet transitions are spin-forbidden and are marked with an 'f' in Table 3. We would not expect any intensity from these transitions in the experimental spectra. Each of the singlet–singlet transitions has finite oscillator strength, but the lowest energy absorption peaks are all

Table 3
Computed singlet and triplet transitions for $CF_3(CF_2)_xCH_2CH_2OH$ ($x = 0,3,5$)

$CF_3CH_2CH_2OH$ ($C_1/^1A$)			$CF_3(CF_2)_3CH_2CH_2OH$ ($C_1/^1A$)			$CF_3(CF_2)_5CH_2CH_2OH$ ($C_1/^1A$)		
Upper state	λ_{calc} (nm)	Oscillator strength	Upper state	λ_{calc} (nm)	Oscillator strength	Upper state	λ_{calc} (nm)	Oscillator strength
^3A	175.8	f	^3A	177.0	f	^3A	177.6	f
^1A	170.6	0.0114	^1A	172.0	0.0051	^1A	173.0	0.0060
^3A	161.6	f	^3A	162.2	f	^3A	166.9	f
^1A	158.7	0.0057	^1A	160.2	0.0053	^1A	165.5	0.0215
^3A	154.1	f	^3A	157.4	f	^3A	162.7	f
^1A	152.9	0.0259	^1A	156.3	0.0082	^1A	161.6	0.0151
^3A	150.0	f	^3A	155.6	f	^3A	159.5	f
^1A	149.5	0.0080	^1A	153.4	0.0376	^1A	157.0	0.0083
^3A	142.8	f	^3A	152.2	f	^3A	153.4	f
^1A	141.5	0.0031	^1A	151.5	0.0081	^1A	152.4	0.0153
^3A	141.1	f	^3A	149.3	f	^3A	151.4	f
^1A	140.2	0.0051	^1A	148.6	0.0139	^1A	149.9	0.0072

below 175 nm. Since this is more than 100 nm below the critical threshold of 290 nm, we can conclude that atmospheric photolysis plays no role for the FTOHs.

Strong absorption is predicted to occur at wavelengths below 175 nm and multiple peaks are predicted in the range from 175 to 140 nm. For $CF_3CH_2CH_2OH$, the strongest absorption peak is predicted to occur at 152.9 nm with oscillator strength of 0.0259. $F(CF_2CF_2)_2CH_2CH_2OH$ is predicted to absorb strongest at 153.4 nm (0.0376), while for $F(CF_2CF_2)_3CH_2CH_2OH$, the largest peak is at 165.5 nm (0.0215).

3.4. Calculated IR spectra

The ab initio calculation of vibrational normal modes and the corresponding harmonic vibrational frequencies has become routine. In this and previous work, we have followed the recommendation of Scott and Radom [43] which was shown to give a root mean square error of 34 cm^{-1} for a set of 122 molecules and 1066 experimental vibrational frequencies. In our earlier paper [37] on the infrared spectra of the perfluorinated aldehydes, $C_xF_{2x+1}CHO$ ($x = 1, 4$), we found that for those transitions for which both experimental and theoretical data exist, the root mean square error was 24 cm^{-1} and the maximum absolute error was 54 cm^{-1}.

Table 4 shows the experimentally observed vibrational bands and the corresponding computed vibrational counterparts. Only those bands with calculated infrared intensities greater than 10 km/mol are shown in Table 4. The complete set of calculated bands are provided as supplementary material.

In Fig. 4, we show simulated IR spectra of $CF_3CH_2CH_2OH$, $F(CF_2CF_2)_2CH_2CH_2OH$, $F(CF_2CF_2)_3CH_2CH_2OH$ and $F(CF_2CF_2)_4CH_2CH_2OH$ in the region 600–1600 cm^{-1}. The theoretical spectral peaks have been artificially broadened with Lorentzian lineshape functions of half-width at half-maximum of 10 cm^{-1} to allow comparison with the corresponding experimental spectra. The details of the following discussion may change somewhat for different broadening linewidths, but the dominant themes will remain unchanged.

The calculated IR spectrum of $CF_3CH_2CH_2OH$ is quite distinct from those of the higher FTOHs. Two intense peaks at 1112 and 1134 cm^{-1} overlap and form the largest structure in the calculated spectrum near 1113 cm^{-1}. A cluster of three peaks at 1224, 1236 and 1269 cm^{-1} form the second largest spectral feature and a substantially less intense cluster of three peaks at 1359, 1365 and 1396 cm^{-1} contribute to a smaller, complex spectral feature. In contrast, the higher fluorinated alcohols have their highest IR absorbance near 1220 cm^{-1} and the peak absorbance is substantially higher when compared to that of $CF_3CH_2CH_2OH$. For $F(CF_2CF_2)_2CH_2CH_2OH$, two overlapping peaks at 1207 and 1216 cm^{-1} produce a very large structure near 1214 cm^{-1}. The second largest peak occurs at 1115 cm^{-1} and a smaller feature at 1174 cm^{-1} lies midway between these larger peaks. For $F(CF_2CF_2)_3CH_2CH_2OH$, these same three features appear. Two overlapping peaks at 1221 and 1236 cm^{-1} contribute a corresponding very high absorbance feature to the spectrum at 1221 cm^{-1}. A peak near 1121 cm^{-1} is somewhat less intense that the corresponding peak for $F(CF_2CF_2)_2CH_2CH_2OH$ and the small midpoint feature at 1174 cm^{-1} in the spectrum of $F(CF_2CF_2)_2CH_2CH_2OH$ appears as a much stronger overlapping pair of peaks near 1179 cm^{-1}. Finally, for the $F(CF_2CF_2)_4CH_2CH_2OH$, the midpoint spectral feature at 1190 cm^{-1} is now of comparable strength to the largest peak at 1221 cm^{-1}.

Comparing Figs. 3 and 4, we see that theory and experiment agree quite well. Experimentally and theoretically, the spectra of the higher fluorinated alcohols quite strongly resemble one another and are quite distinct from the spectrum of $CF_3CH_2CH_2OH$. Theory and experiment have the highest absorbance peaks in the same location and the relative intensities of the major spectral features correspond reasonably well. There are two points of significant disagreement. As one proceeds from $F(CF_2CF_2)_2CH_2CH_2OH$ to $F(CF_2CF_2)_4CH_2CH_2OH$, the relative strengthening of the middle peak near 1175 cm^{-1} is more pronounced

Table 4
Observed and calculated[a] vibrational bands (cm^{-1}), calculated infrared intensities (km/mol), and approximate band assignments for $CF_3(CF_2)_xCH_2CH_2OH$ ($x = 0, 3, 5, 7$)

$CF_3CH_2CH_2OH$			$CF_3(CF_2)_3CH_2CH_2OH$			$CF_3(CF_2)_5CH_2CH_2OH$			$CF_3(CF_2)_7CH_2CH_2OH$		
ν_{obs}	ν_{calc}	IR intensity	ν_{obs}	ν_{calc}	IR intensity	ν_{obs}	ν_{calc}	IR intensity	ν_{obs}	ν_{calc}	IR intensity
	360	24.7		389[b]	125.9		258	10.5		386[b]	132.7
	388[b]	115.5		432	30.8		396[b]	120.9		438	60.7
	458	17.2		443	20.0		434	57.3		498	12.4
	522	12.2		495	10.4		495	10.2		502	21.9
871	856	14.6		564	14.8		501	14.6		529	27.0
948	916	10.0		683	66.7		536	21.4		548	48.0
1010	992	51.4	715	717	16.4		576	10.1		575	14.7
1046	1050	43.4		799	79.2	653	626	79.7		629	22.9
1139	1112	262.8	882	859	27.3	699	672	125.2	658	632	197.2
	1134	110.5	1006	984	39.7		708	11.8		673	23.4
1224	1207	126.6	1045	1023	33.7		739	23.0		914	11.2
1260	1236[c]	120.5		1053	84.8		834	12.7		944	37.4
	1269[d]	65.5		1106	99.7		921	11.0		990	36.8
	1359	35.3	1140	1115	199.9		987	29.5		1034	52.7
1378	1365	46.3		1143	39.4	1043	1054	142.6	1046	1056	58.4
	1396	45.3		1148	15.2		1097	52.0		1090	49.6
1440	1440[e]	12.9		1164	24.9	1126	1107	68.7	1120	1107	66.0
	2900[f]	49.3		1174	152.7		1121	167.9		1110	48.8
	2996[f]	28.5		1207	211.4		1140	23.1	1139	1128	265.4
	3011[g]	10.0	1246	1216	343.9		1145	73.8		1138	23.7
	3612[h]	34.0		1241	104.0		1159	30.7		1144	14.9
				1258[d]	50.1	1151	1162	151.3		1150	35.9
				1269	14.7		1170	95.0		1156	12.0
			1358	1320	60.8	1216	1181	206.2		1165	110.1
				1350[j]	21.3		1191	59.3	1158	1175	112.7
				1392	58.6		1216	60.1		1186	75.8
				2905[f]	46.7	1251	1221	464.3	1223	1190	399.6
				2996[f]	27.7		1236	117.8		1202	56.7
				3618[h]	31.5		1256[d]	32.3		1214	145.8
							1267	22.1	1253	1223	498.1
							1283	46.9		1246	20.4
							1327	51.9		1254[d]	41.2
							1350[i]	23.6		1258	50.0
						1367	1393	64.5		1294	59.4
							2904[f]	46.5		1331	44.4
							2996[f]	27.9		1350[i]	24.9
							3619[h]	31.1	1369	1393	68.0
										2909[f]	46.2
										2995[f]	28.0
										3617[h]	30.5

[a] Table contains those bands with calculated intensities greater than or equal to 10 km/mol.
[b] H–O-C out of plane bend.
[c] Mix of methylene twist and wag.
[d] Methylene twist.
[e] H–C–H scissors bend.
[f] C–H stretch.
[g] C–H asymmetric stretch.
[h] O–H stretch.
[i] Methylene wag.

in the calculated spectra than the experimental spectra. In addition, low absorbance features in the experimental spectra of $CF_3CH_2CH_2OH$ (665 cm^{-1}), $F(CF_2CF_2)_2CH_2CH_2OH$ (748 cm^{-1}) and $F(CF_2CF_2)_4CH_2CH_2OH$ (705 cm^{-1}) have no counterparts in the theoretical spectra. Otherwise, we were able to associate all the experimental peaks with corresponding peaks in the simulated spectra.

Experimental and scaled theoretical vibrational frequencies show good agreement. Taking all four molecules together, for the 32 transitions for which both experimental and theoretical data exist, the root mean square error is 17 cm^{-1} and the maximum absolute error is 38 cm^{-1}. This degree of agreement is typical for this level of theoretical treatment. Examining the molecules individually, the root

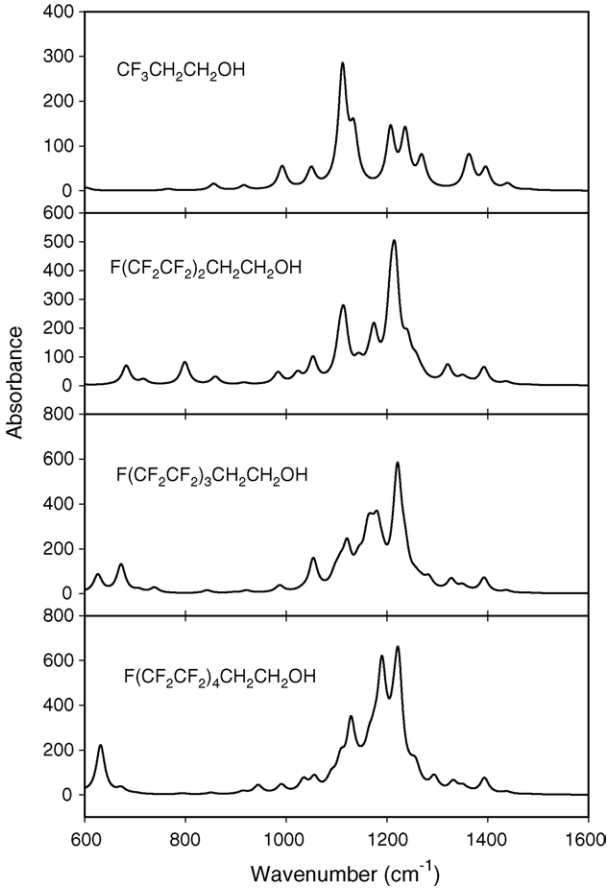

Fig. 4. Computed IR spectra of $CF_3CH_2CH_2OH$, $F(CF_2CF_2)_2CH_2CH_2OH$, $F(CF_2CF_2)_3CH_2CH_2OH$ and $F(CF_2CF_2)_4CH_2CH_2OH$. The lines have been artificially broadened with a Lorentzian lineshape (full width at half-maximum of 20 cm^{-1}).

mean square and maximum absolute errors are, respectively, 12 and 32 cm^{-1} for $CF_3CH_2CH_2OH$, 12 and 38 cm^{-1} for $F(CF_2CF_2)_2CH_2CH_2OH$, 23 and 35 cm^{-1} for $F(CF_2CF_2)_3$-CH_2CH_2OH and 20 and 33 cm^{-1} for $F(CF_2CF_2)_4CH_2$-CH_2OH. There is a clear tendency for theory to slightly underpredict the location of the experimental IR bands. The scaled theoretical frequencies are lower for 25 of the 32 transitions listed in Table 4.

By visual inspection of each computed normal mode, we have attempted to describe the character of the modes in terms of stretching and bending deformations. These descriptions are approximate and the true normal modes usually involve a complicated mixture of atomic motions. In particular, the largest absorbance peaks of the FTOHs at 1113 cm^{-1} ($CF_3CH_2CH_2OH$) and near 1220 cm^{-1} ($F(CF_2CF_2)_xCH_2CH_2OH$ ($x = 2$, 3, 4)) correspond to complex mixtures of backbone bends, C–F and C–H bond stretches. Each successive addition of two CF_2 units adds 18 new low frequency normal modes. These modes are difficult to analyze, but appear to be strongly coupled backbone bends and symmetric and asymmetric C–F bond stretches.

4. Summary

A comprehensive study of the UV and IR spectra of fluorotelomer alcohols has been presented. Experimental and computational results obtained in three different laboratories were consistent giving high confidence in the results. The UV spectra show that photolysis will not be a significant loss mechanism for these compounds. Weak intramolecular hydrogen bonding is predicted in the gas phase; in the condensed phase, this bonding will be overwhelmed by strong intermolecular hydrogen bonding. The IR spectra reported herein should aid in future laboratory and field studies of the atmospheric chemistry of these species. Finally, the FTOHs have negligible global warming potentials due to their short atmospheric lifetimes [3,46].

Acknowledgements

S.M.L. Melo and K. Strong wish to thank Prof. James R. Drummond and the NSERC Industrial Research Chair in Atmospheric Remote Sounding from Space (sponsored by COMDEV, Bomem, AES (MSC), CSA and NSERC) for the use of the Bomem DA8 Fourier transform spectrometer, and D. Barclay, G. Chang, P. Chen and M. Toohey for their contributions to the experimental setup. Work at the University of Toronto was supported through funds from NSERC and an NSERC Strategic grant to S.A. Mabury. In addition, R.L. Waterland would like to thank Robert C. Buck and Mary A. Kaiser for their review of the manuscript.

Appendix A. Supplementary data

Supplementary data associated with this article can be found, in the online version, at doi:10.1016/j.jfluchem.2005.06.010.

References

[1] J.W. Martin, D.C.G. Muir, W.C. Kwan, C.A. Moody, K.R. Solomon, S.A. Mabury, Anal. Chem. 74 (2002) 584.
[2] J.W. Martin, M.M. Smithwick, B. Braune, P.F. Hoekstra, D.C.G. Muir, S.A. Mabury, Environ. Sci. Technol. 38 (2004) 373.
[3] D.A. Ellis, J.W. Martin, S.A. Mabury, M.D. Hurley, M.P. Sulbaek Andersen, T.J. Wallington, Environ. Sci. Technol. 37 (2003) 3816.
[4] D.A. Ellis, J.W. Martin, A.O. De Silva, S.A. Mabury, M.D. Hurley, M.P. Sulbaek Andersen, T.J. Wallington, Environ. Sci. Technol. 38 (2004) 3316.
[5] M.D. Hurley, J.C. Ball, M.P. Sulbaek Andersen, T.J. Wallington, D.A. Ellis, J.W. Martin, S.A. Mabury, J. Phys. Chem. A 108 (2004) 5635.
[6] S. Pinnock, K.P. Shine, T.J. Smyth, M.D. Hurley, T.J. Wallington, J. Geophys. Res. 100 (1995) 23227.
[7] N.L. Stock, D.A. Ellis, L. Deleebeeck, D.C.G. Muir, S.A. Mabury, Environ. Sci. Technol. 38 (2004) 1693.

[8] Y.D. Lei, F. Wania, D. Mathers, S.A. Mabury, J. Chem. Eng., Data 49 (2004) 1013.
[9] P.J. Krusic, A.A. Marchione, F. Davidson, M.A. Kaiser, C.C. Kao, R.E. Richardson, M. Botelho, R.L. Waterland, R.C. Buck, J. Phys. Chem., A 123 (2005) 6232.
[10] The nomenclature n-2 FTOH specifies the number of fluorinated and hydrogenated carbons in the molecule (e.g. 8-2 FTOH for CF3-(CF_2)7-CH_2-CH_2-OH).
[11] F.C. Marler III, H.P. Hopkins Jr., J. Phys. Chem. 74 (1970) 4164.
[12] D.A. Dixon, B.E. Smart, J. Phys. Chem. 95 (1991) 1609.
[13] P.J. Kruger, H.D. Mattee, Can. J. Chem. 42 (1964) 326.
[14] K.B. Wiberg, M.A. Murcko, THEOCHEM 40 (1988) 1.
[15] I. Bako, T. Radnai, F. Bellisent, Claire Marie, J. Chem. Phys. 121 (2004) 12472.
[16] C.R.S. Briggs, M.J. Allen, D. O'Hagen, D.J. Tozer, A.M.Z. Alexandra, A.E. Goeta, J.A.K. Howard, Org. Biomol. Chem. 2 (2004) 732.
[17] A. Kovas, I. Macsari, I. Hargittai, J. Phys. Chem. A 103 (1999) 3110.
[18] G.L. Carlson, W.G. Fately, A.S. Manocha, F.F. Bentley, J. Phys. Chem. 76 (1972) 1553.
[19] J. Cizek, J. Chem. Phys. 45 (1966) 4256.
[20] M. Head-Gordon, J. Phys. Chem. 100 (1996) 13220.
[21] M. Sprik, J. Hutter, M. Parinello, J. Chem. Phys. 105 (1996) 1142.
[22] M. Makowski, J. Makowska, L. Chmurzynski, THEOCHEM 674 (2004) 61.
[23] B. Paizs, S. Suhai, J. Comp. Chem. 19 (1998) 575.
[24] P.R. Rablen, J.W. Lockman, W.L. Jorgensen, J. Phys. Chem. A 102 (1998) 3782.
[25] P.J. Stevens, J.F. Devlin, C.F. Chabalowski, M.J. Frisch, J. Phys. Chem. 98 (1994) 11623.
[26] The basis sets 6-31+G(d(X+),p) and 6-31++G(2d(X+),p) include additional diffuse polarization functions only on atoms having lone pairs.
[27] Gaussian 03, Revision B.05, M.J. Frisch, G.W. Trucks, H.B. Schlegel, G.E. Scuseria, M.A. Robb, J.R. Cheeseman, J.A. Montgomery, Jr., T. Vreven, K.N. Kudin, J.C. Burant, J.M. Millam, S.S. Iyengar, J. Tomasi, V. Barone, B. Mennucci, M. Cossi, G. Scalmani, N. Rega, G.A. Petersson, H. Nakatsuji, M. Hada, M. Ehara, K. Toyota, R. Fukuda, J. Hasegawa, M. Ishida, T. Nakajima, Y. Honda, O. Kitao, H. Nakai, M. Klene, X. Li, J.E. Knox, H.P. Hratchian, J.B. Cross, C. Adamo, J. Jaramillo, R. Gomperts, R.E. Stratmann, O. Yazyev, A.J. Austin, R. Cammi, C. Pomelli, J.W. Ochterski, P.Y. Ayala, K. Morokuma, G.A. Voth, P. Salvador, J.J. Dannenberg, V.G. Zakrzewski, S. Dapprich, A.D. Daniels, M.C. Strain, O. Farkas, D.K. Malick, A.D. Rabuck, K. Raghavachari, J.B. Foresman, J.V. Ortiz, Q. Cui, A.G. Baboul, S. Clifford, J. Cioslowski, B.B. Stefanov, G. Liu, A. Liashenko, P. Piskorz, I. Komaromi, R.L. Martin, D.J. Fox, T. Keith, M.A. Al-Laham, C.Y. Peng, A. Nanayakkara, M. Challacombe, P.M.W. Gill, B. Johnson, W. Chen, M.W. Wong, C. Gonzalez, J.A. Pople, Gaussian Inc., Pittsburgh, PA, 2003.
[28] M.E. Casida, C. Jamorski, K.C. Casida, D.R. Salahub, J. Chem. Phys. 108 (1998) 4439.
[29] C. Jamorski, M.E. Casida, D.R. Salahub, J. Chem. Phys. 104 (1999) 5134.
[30] M.E. Casida, D.R. Salahub, J. Chem. Phys. 113 (2000) 8918.
[31] C. Adamo, G.E. Scuseria, V. Barone, J. Chem. Phys. 111 (1999) 2889.
[32] K.B. Wiberg, R.E. Stratmann, M.J. Frisch, Chem. Phys. Lett. 297 (1998) 60.
[33] Z.-L. Cai, J.R. Reimers, J. Chem. Phys. 112 (2000) 527.
[34] S.J.A. van Gisbergen, J.A. Groeneveld, A. Rosa, J.G. Snijders, E.J. Baerends, J. Phys. Chem. A 103 (1999) 6835.
[35] J.B. Foresman, M. Head-Gordon, J.A. Pople, M.J. Frisch, J. Phys. Chem. 96 (1992) 135.
[36] (a) N.N. Matsuzawa, A. Ishitani, D.A. Dixon, T. Uda, J. Phys. Chem. A 105 (2001) 4953;
(b) N.N. Matsuzawa, S. Mori, E. Yano, S. Okazaki, A. Ishitani, D.A. Dixon, Proc. SPIE 3999 (2000) 375;
(c) N.N. Matsuzawa, A. Ishitani, D.A. Dixon, T. Uda, Proc. SPIE 4345 (2001) 396;
(d) D.A. Dixon, N.N. Matsuzawa, A. Ishitani, T. Uda, Physica Status Solidi B Appl. Res. 226 (2001) 69;
(e) N. Matsuzawa, A. Ishitani, C.-G. Zhan, D.A. Dixon, T. Uda, J. Fluor. Chem. 122 (2003) 27.
[37] R.L. Waterland, K.D. Dobbs, A.M. Rinehart, A.E. Feiring, R.C. Wheland, B.E. Smart, J. Fluor. Chem. 122 (2003) 37.
[38] Y. Hashikawa, M. Kawasaki, R.L. Waterland, M.D. Hurley, J.C. Ball, T.J. Wallington, M.P. Sulbaek Andersen, O.J. Nielsen, J. Fluor. Chem. 125 (2004) 1925.
[39] A.D. Becke, J. Chem. Phys. 98 (1993) 5648.
[40] C. Lee, W. Yang, R.G. Parr, Phys. Rev. B 37 (1988) 785.
[41] N. Godbout, D.R. Salahub, J. Andzelm, E. Wimmer, Can. J. Chem. 70 (1992) 560.
[42] T.H. Dunning, P.J. Hay, in: H.F. Schaefer, III (Ed.), Methods of Electronic Structure Theory, 3, Plenum Press, New York, 1977.
[43] A.P. Scott, L. Radom, J. Phys. Chem. 100 (1996) 16502.
[44] S. Pinnock, K.P. Shine, T.J. Smyth, M.D. Hurley, T.J. Wallington, J. Geophys. Res. 100 (1995) 23227.
[45] (a) For comparison, the H-bond strength of ethanol dimers is ~5 kcal/mol, see for example
(b) W.O. George, T. Has, M.F. Hossain, B.F. Jones, R. Lewis, J. Chem. Soc., Faraday Trans. 94 (1988) 2701–2708.
[46] T. Kelly, V. Bossoutrot, I. Magneron, K. Wirtz, J. Treacy, A. Mellouki, H. Sidebottom, G. Le Bras, J. Phys. Chem. A 109 (2005) 347.